

# MACHINE UNLEARNING FOR CONTRASTIVE LEARNING UNDER AUDITING

**Anonymous authors**

Paper under double-blind review

## ABSTRACT

Machine unlearning offers effective solutions for revoking the influence of specific training data on pre-trained model parameters. While existing approaches address unlearning for classification and generative models, they overlook an important category of machine learning models: contrastive learning (CL) methods. This paper addresses this gap by introducing the Machine Unlearning for Contrastive Learning (MUC) framework and adapting existing methods. We identify limitations in current approaches, noting that several methods perform inadequately as unlearners and that existing auditing tools insufficiently validate unlearning effects in contrastive learning. To address these issues, we propose Alignment Calibration (AC), a novel method that explicitly considers contrastive learning properties and optimizes towards new auditing metrics for easy verification of unlearning. Through empirical comparisons with baseline methods on SimCLR, MoCo, and CLIP, we demonstrate that AC: (1) achieves state-of-the-art performance, approximating exact unlearning (retraining); (2) enables data owners to clearly visualize unlearning effects through *black-box auditing*.

## 1 INTRODUCTION

The success of modern machine learning models largely relies on training with a large corpus of data. However, carefully annotated data are expensive and difficult to obtain, thus urging the utilization of the vast amount of unlabeled data in the wild. The recent self-supervised learning methods, especially contrastive learning methods (Chen et al., 2020; 2021; He et al., 2020), provide viable solutions to learning general representations for various downstream tasks. For example, unimodal contrastive learning models employ the InfoNCE loss to maximize the feature similarity between positive pairs (e.g., different data augmentations of the same image) while minimizing that between the negative ones (e.g., different images). This training scheme also applies to multi-modal training (e.g., CLIP (Radford et al., 2021)), and the learned encoders are widely applied in various tasks, e.g., GPT-based models (Achiam et al., 2023) and latent diffusion models (Rombach et al., 2022).

To amass large-scale datasets for training contrastive learning models, practitioners often resort to web crawling (e.g., using Common Crawl<sup>1</sup>). However, such data collection methods may disregard data owners’ privacy concerns, potentially retrieving their data without consent. Moreover, acquired training data may include copyrighted material or even inappropriate content, such as sexual abuse (e.g., in recent reports<sup>2</sup> against content in LAION-5B (Schuhmann et al., 2022)). In these scenarios, data owners or authorities may rightfully request the removal of misused training data (*i.e.*, unlearning dataset)<sup>3</sup>, necessitating adjustments to the trained model parameters. While retraining the model from scratch without the unlearning dataset is a straightforward solution, it incurs substantial computational costs for large models and datasets.

To eliminate the effect of the unlearning dataset on the model with minimum effort, machine unlearning methods (Cao & Yang, 2015; Bourtole et al., 2021; Ginart et al., 2019; Guo et al., 2019; Neel et al., 2021; Ullah et al., 2021; Sekhari et al., 2021; Izzo et al., 2021; Chen et al., 2023; Zhang

<sup>1</sup><https://commoncrawl.org/>

<sup>2</sup><https://purl.stanford.edu/kh752sm9123>

<sup>3</sup>In accordance with policies such as the European Union’s General Data Protection Regulation (GDPR), the California Consumer Privacy Act (CCPA), and Canada’s proposed Consumer Privacy Protection Act (CPPA).

054  
055  
056  
057  
058  
059  
060  
061  
062  
063  
064  
065  
066  
067  
068  
069  
070  
071  
072  
073  
074  
075  
076  
077  
078  
079  
080  
081  
082  
083  
084  
085  
086  
087  
088  
089  
090  
091  
092  
093  
094  
095  
096  
097  
098  
099  
100  
101  
102  
103  
104  
105  
106  
107

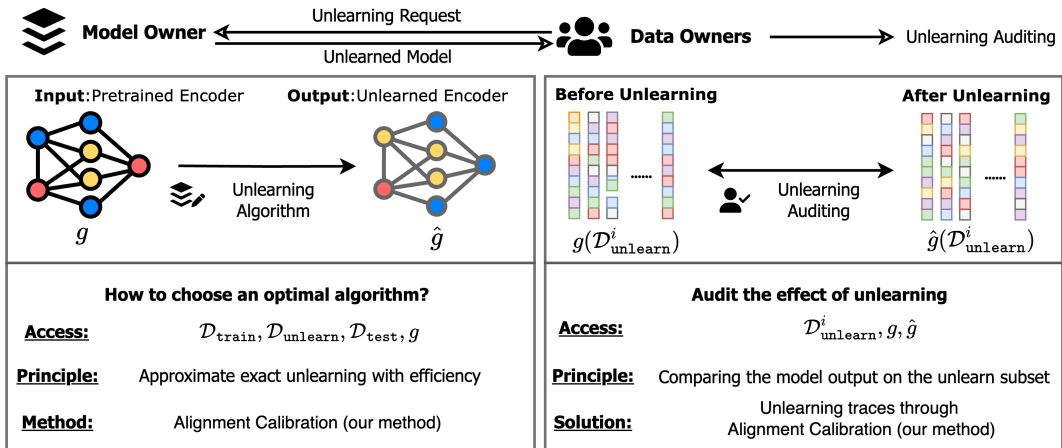


Figure 1: An overview of the unlearning pipeline for contrastive learning. Given a training set  $D_{\text{train}}$  contains an unlearn subset  $D_{\text{unlearn}}$ , and a pretrained encoder  $g$ , model owners (Column 1) aim to find an optimal unlearning algorithm by comparing with exact unlearning (retraining with the retain dataset  $D_{\text{train}} \setminus D_{\text{unlearn}}$ ) to obtain an unlearned encoder  $\hat{g}$ . Data owners (Column 2), who only have *black-box* access to the model outputs, then audit the unlearning outcome by comparing the output features before/after unlearning.

et al., 2024a; Fan et al., 2024; Shen et al., 2024) provide recipes for supervised learning methods on group removal and for generative models on sample or concept removal. However, the study of an efficient solution for contrastive learning models is under-explored. In this paper, we establish the foundation of **Machine Unlearning for Contrastive Learning models (MUC)**. MUC adapts various existing methods to contrastive learning and introduces the notion of data owners who request unlearning and model owners who execute unlearning. Given candidate unlearning algorithms, the model owners first perform *white-box evaluation* to select the best method and generate an optimal unlearned model. The data owners then perform *black-box auditing* to validate the effect of the unlearning procedure. We argue that unlearning success is achieved only if the unlearned model meets the criteria on both sides. We summarize this unlearning pipeline in Figure 1.

Unfortunately, direct adaptations of existing unlearning approaches are unsatisfactory on both considerations. Firstly, from the model owners’ perspective, such algorithms are suboptimal approximations of exact unlearning (training from scratch) under different white-box evaluations and there lack of a good candidate method. Secondly, from the data owner’s perspective, even given an optimal unlearned model, it is difficult to discern the unlearning effect under existing *black-box auditing* tools, rendering it hard to determine the success of unlearning.

Motivated by the above state of affairs, we introduce a novel unlearning method called *Alignment Calibration (AC)* that is specifically tailored for contrastive learning. AC optimizes a novel loss function that involves three terms: (1) a positive alignment calibration term that removes the footprint of the unlearn set on the representation; (2) a negative alignment calibration term that leaves explicit unlearning traces for auditing; (3) a performance preserving term that maintains uniformity.

Finally, we empirically compare baseline methods with our *Alignment Calibration* algorithms on unlearning models pre-trained on SimCLR (Chen et al., 2020) MoCo (He et al., 2020), and CLIP (Radford et al., 2021). Under various unlearning settings (e.g., the fraction of the unlearning dataset) and evaluation metrics, AC consistently outperforms the baseline methods, especially under unlearn auditing, validating the benefits of our method. In summary, we make the following contributions:

- We propose the MUC framework that considers existing methods and various evaluation tools in contrastive learning, including *white-box evaluation* and *black-box auditing*.
- Motivated by insufficiencies of existing unlearning algorithms and auditing tools, we propose the novel *Alignment Calibration* method that satisfies both model owners and data owners.
- Our experiments initiate the evaluation of existing machine unlearning methods for contrastive learning and confirm the superiority of our new methods.

## 2 BACKGROUND AND RELATED WORK

We first provide background and related work on contrastive learning and machine unlearning.

**Contrastive Learning and Self-supervised Learning** Contrastive learning learns general representations by contrasting sample pairs (usually without labels), which analytically benefits the downstream applications (Saunshi et al., 2019; Tosh et al., 2021). Popular contrastive learning methods such as Contrastive Predictive Coding (CPC) (van den Oord et al., 2018), SimCLR (Chen et al., 2020), and MoCo (He et al., 2020) employ the InfoNCE loss to enforce the contrast between positive and negative pairs. Other variants of the InfoNCE-based loss are also widely applied, e.g.,  $\hat{f}$ -MICL (Lu et al., 2023), Alignment and Uniformity (Wang & Isola, 2020), and Pearson  $\chi^2$  divergence (Tsai et al., 2021). This contrastive training scheme is also applied to the context of multimodal learning, where images and texts are formed as pairs, e.g., in CLIP (Radford et al., 2021). There exist other self-supervised learning methods that also learn representations (Grill et al., 2020; Chen & He, 2021; He et al., 2022; Caron et al., 2021). In this paper, we mainly focus on developing unlearning recipes for contrastive learning methods, especially SimCLR, MoCo, and CLIP.

Specifically, contrastive learning usually applies the InfoNCE loss to learn a representation  $g$ . Given a probability measure  $p$ , we define the density of *positive pairs* sampled from  $p$  as  $p^+$ , i.e., two samples with similar feature embeddings as the joint distribution; and the density of *negative pairs* as  $p^-$ . Specifically, one minimizes the loss below as the objective:

$$L_{\text{InfoNCE}} = -\mathbb{E}_{(x,y) \sim p^+} \log \mathbb{E}_{y \sim p^-} \exp(s(g(x); g(y))) ; \quad (1)$$

where  $s$  is the cosine similarity after normalization with a temperature parameter, and  $g(x); g(y)$  are the features extracted by a given encoder  $g$ , respectively. The above contrastive learning (pre-training) scheme learns a general encoder  $g$  (image and text encoders for CLIP). Such a (fixed)  $g$  can be utilized with an additional linear head or shallow models for downstream tasks. In this paper, we mainly consider linear probing, where  $g$  is used for the classification of the same dataset with pretraining. Notably, we consider unlearning during the pretraining phase only.

**Machine Unlearning** *For Supervised Learning:* Machine unlearning (MU) (Cao & Yang, 2015) requires an algorithm to revert to a state that specific data points are never trained on. While exact unlearning (Bourtoule et al., 2021) (e.g., retraining the model entirely on the `retain` dataset) provides a reliable solution, the additional computation requirement is also tremendous. In this paper, we focus on **approximate unlearning** (Ginart et al., 2019; Guo et al., 2019; Neel et al., 2021; Ullah et al., 2021; Sekhari et al., 2021; Izzo et al., 2021; Chen et al., 2023; Zhang et al., 2024a; Fan et al., 2024; Shen et al., 2024) to efficiently achieve the same goal.

*For Generative Models:* MU methods are applied to diffusion models to avoid copyright infringement and inappropriate image generation (Gandikota et al., 2023; Zhang et al., 2023b; Heng & Soh, 2023; Kumari et al., 2023). For large language models, MU is applied as a model-editing (Yao et al., 2023) tool to enable forgetting on certain training texts (Mitchell et al., 2022b;a; Jang et al., 2022; Eldan & Russinovich, 2023; Zhang et al., 2023a; Hu et al., 2024; Jia et al., 2024; Maini et al., 2024; Liu et al., 2024; Zhang et al., 2024b). In this paper, we focus on MU on self-supervised learning, specifically, contrastive learning methods, which differs from the above two cases in both unlearning settings and frameworks, which we specify in the following section.

## 3 MACHINE UNLEARNING FOR CONTRASTIVE LEARNING (MUC)

In this section, we specify the problem setting of machine unlearning for contrastive learning, introduce direct adaptations of existing methods, and propose evaluation metrics.

### 3.1 PROBLEM SETTINGS

**Formal Notations:** (1) We denote the pretrained encoder as  $g$  and the encoder after unlearning as  $\hat{g}$ . Given an input sample  $x$ , the features extracted by the encoders are denoted as  $g(x)$  and  $\hat{g}(x)$  respectively; (2) We denote the original training set as  $D_{\text{train}}$  (which is used to train  $g$ ), the unlearn set as  $D_{\text{unlearn}}$  and the retain set as  $D_{\text{retain}} = D_{\text{train}} \setminus D_{\text{unlearn}}$  ( $\setminus$  denotes removal here); (3) We

define two parties involved in unlearning: the model owner who receives the unlearning request, and the data owner who wishes to remove data. In practical scenarios, consist of a group of individuals  $\mathcal{F} = \{g_{i=1}^N\}$ , who may not know the existence of each other, but participate in unlearning at the same time.

**Approximate Unlearning:** The model owner aims at choosing an unlearning algorithm that approximates exact unlearning (training on  $D_{\text{retain}}$  from scratch) to obtain  $\hat{g}$ . In the meantime, this algorithm should be much more efficient than exact unlearning. Given a pool of candidate algorithms, performs *white-box evaluations* (access to  $D_{\text{train}}; D_{\text{unlearn}}; D_{\text{test}}; g$  and candidates  $f(\hat{g})$ ) by comparing their performances with exact unlearning according to metrics in Section 3.3.

**Unlearning Auditing:** Assuming the unlearning process is finished and the model owner has published the final unlearned model  $\hat{g}$ , an individual data owner  $i$  wishes to examine the unlearning outcome. We coin this process as **unlearning auditing**. Specifically, such auditing is *black-box* as  $i$  only has access to his/her own unlearning subset  $D_{\text{unlearn}}^i$ , and the output of the model before  $g(D_{\text{unlearn}}^i)$  and after unlearning  $\hat{g}(D_{\text{unlearn}}^i)$ . By comparing these outputs,  $i$  should find explicit evidence that unlearning has indeed been performed and the output is as desired. Our paper aims to provide such evidence through the design of a novel unlearning algorithm for contrastive learning.

Note that making unlearning auditable is an important and difficult task for approximate unlearning algorithms (Thudi et al., 2022). While we provide easy-to-check unlearning traces in the later sections, such tools are specifically designed for our algorithm in contrastive learning, and may not be generalized to other unlearning scenarios.

### 3.2 ADAPTING EXISTING METHODS TO MUC

We first adapt some existing unlearning methods designed for supervised unlearning to contrastive unlearning. Due to the lack of labels in contrastive learning pre-training, some approaches cannot be directly applied. For example, random labeling (Golatkar et al., 2020; Fan et al., 2024) relies on flipping the labels of the unlearn data; boundary unlearning (Chen et al., 2023) expands or shrinks the decision boundary, which does not exist in our context. In contrast, some other unlearning methods can be tailored to contrastive learning. Specifically, we adapt the following methods:

- *Retraining*: (exact unlearning) trains on  $D_{\text{retain}}$  from scratch via minimizing Equation (1);
- *Fine-tuning* (Golatkar et al., 2020) updates the pre-trained model for several epochs on  $D_{\text{retain}}$ ;
- *Gradient Ascent* (Golatkar et al., 2020; Neel et al., 2021; Thudi et al., 2022) reversely maximizes Equation (1) on the  $D_{\text{unlearn}}$ ;
- *NegGrad* (Kurmanji et al., 2023) jointly minimizes and maximizes Equation (1) on  $D_{\text{retain}}$  and  $D_{\text{unlearn}}$  respectively;
- $\ell_1$ -*Sparsity* (Jia et al., 2023) regularizes the  $\ell_1$ -norm of model parameters based on fine-tuning.

The above methods manifest straightforward adaptations of unlearning from supervised learning to contrastive learning by changing the cross entropy loss to the InfoNCE loss in Equation (1). In Section 5, we show that approximate unlearning methods are suboptimal approximations of exact unlearning, namely that there still exists a performance gap compared with retraining. This motivates us to design new unlearning methods specifically for contrastive learning in Section 4.

### 3.3 HOW TO CHOOSE AN UNLEARNING ALGORITHM

Suppose the model owner gathers a pool of unlearning algorithms (e.g., the methods above). Next we introduce how to compare them, *i.e.*, the evaluation metrics. As contrastive learning returns a feature extractor, we can either evaluate unlearning on the representations directly or rely on downstream tasks. Specifically:

- *Representation-level metrics.* ¶ Forgetting Score: given a candidate algorithm that updates  $g$  to  $\hat{g}$ , we propose a Forgetting Score (FS) by directly adapting the memorization score in evaluating data attribution in Wang et al. (2024). FS measures the quantity of forgetting  $D_{\text{unlearn}}$  by comparing

the alignment loss through the features returned by model parameters before and after unlearning:

$$FS := \mathbb{E}_{(x,y) \sim p_u^+} s(g(x); g(y)) - \mathbb{E}_{(x,y) \sim p_u^+} s(\hat{g}(x); \hat{g}(y)); \quad (2)$$

where  $p_u$  is the density of  $D_{\text{unlearn}}$ , recall  $g$  and  $\hat{g}$  are models before/after unlearning.

• **Membership Inference Attacks (MIA)**: MIAs are capable of indicating whether certain samples (e.g., the unlearn set) are included in the training set and are perfect for examining unlearning efficacy. EncoderMI (Liu et al., 2021) proposed an alignment-based membership inference attack for self-supervised encoders. It extracts membership information from the embedded features to distinguish whether input data is included in the encoder training set. Following the implementation of Jia et al. (2023); Fan et al. (2024), we evaluate the attack success rate (ASR) on the unlearn dataset  $D_{\text{unlearn}}$  and denote it by encoder membership inference attack (**EMIA**) efficacy. We compare EMIA on  $D_{\text{unlearn}}$  with retraining. See Appendix A.3 for details of EMIA.

- **Downstream-level metrics**. Alternatively, representations can be evaluated with downstream tasks. We perform linear probing, *i.e.*, image classification on the same (labeled) dataset for unimodal contrastive learning. Given the unlearned encoder  $\hat{g}$  returned by a candidate algorithm, we train an additional linear head on  $D_{\text{retain}}$  on top of the fixed  $\hat{g}$  to obtain a classifier. Next we evaluate:
  - **Accuracies**: we evaluate retain accuracy (**RA**) on  $D_{\text{retain}}$ , test accuracy on  $D_{\text{test}}$  (**TA**), and unlearn accuracy on  $D_{\text{unlearn}}$  (**UA**). For a good unlearning algorithm, the above three measurements should be close to those of the retrained model, with a common pattern of **UA** < **TA** < **RA**;
  - **Membership Inference Attacks**: Similarly to EMIA, we implement a confidence-based membership inference attack (Jia et al., 2023; Fan et al., 2024; Song & Mittal, 2021) on the entire network (encoder and linear head) and report classifier membership inference attack (**CMIA**) efficacy. We compare CMIA with retraining. See Appendix A.3 for details.

### 3.4 HOW TO AUDIT UNLEARNING

After choosing an optimal unlearning algorithm, the model owner generates the unlearned model  $\hat{g}$  as a response to the unlearning request made by data owners. However, it is impossible for the data owners to perform the same *white-box evaluations*.

**For the data owners (Unlearning Auditing)**: Recall that an individual data owner  $i$  performs *black-box auditing* due to the limited access to input  $D_{\text{unlearn}}^i$  and the output of the encoder before/after unlearning. Specifically,  $i$  cannot train shadow<sup>4</sup> models with  $D_{\text{unlearn}}^i$  alone to perform MIAs; and cannot obtain **TA** or **RA** to quantify performance. Additionally, there is a **lack** of the retrain baseline to compare with. To this end, the only auditing tool is the forgetting score **FS** on  $D_{\text{unlearn}}$ , which can be calculated with Equation (2). However, we argue that this auditing is **neither sufficient nor reliable**, and we use a simple empirical example to validate this claim:

*Exact unlearning on MoCo* (He et al., 2020): We perform exact unlearning (*i.e.*, retraining) to forget 4500 training images of CIFAR-10 (randomly chosen) on MoCo (ResNet-18). We calculate the forgetting score **FS** for every unlearn sample and calculate the mean and the standard deviation across the 4500 unlearning images. We obtain  $\mu = 0.025$ ;  $\sigma = 0.081$ .

Here we observe that the large standard deviation  $\sigma = 0.081 = 3.24 \mu$  makes the current auditing largely unreliable. For individual data owners, if the unlearn subset size  $|D_{\text{unlearn}}^i|$  is small, its corresponding sample-wise **FS** is likely to be biased and the average could fluctuate around 0, suggesting little forgetting. This could lead to the belief that “unlearning hasn’t been performed” from the data owner’s side, thus rejecting the exact unlearned model, as well as any approximate unlearning algorithms, given that “matching exact unlearning” is the criteria for selection. This example reveals the insufficiency of using only **FS** as the unlearn auditing tool in contrastive learning.

In summary, under the current MUC framework, existing approximate unlearning algorithms and auditing tools are insufficient. To address this, we design new unlearning algorithms for the model owners and advanced auditing tools for data owners in contrastive learning in the next section, which would benefit both parties in engaging the unlearning procedure.

<sup>4</sup>Surrogate models to train classifiers for membership inference.

## 4 ALIGNMENT CALIBRATION

### 4.1 TAILORED OBJECTIVE FOR MUC

We first introduce a more effective unlearner for model owners. Recall that’s goal for unlearning is preserving the model utility on  $D_{\text{retain}}$  while revoking the effects of training on  $D_{\text{unlearn}}$ . For the retain dataset  $D_{\text{retain}}$ , we minimize the InfoNCE loss in Equation (1) to achieve reasonable downstream performance after unlearning:

$$L_{\text{retain}} = \mathbb{E}_{(x,y) \sim \rho_r^+} s(g(x); g(y)) + \mathbb{E}_x \log \mathbb{E}_y \exp(s(g(x); g(y))); \quad (3)$$

where  $\rho_r$  is the density of  $D_{\text{retain}}$  and  $\rho_d$  is the density of  $D_{\text{train}}$ .

For the unlearn dataset  $D_{\text{unlearn}}$ , revoking the effects of training amounts to achieving the following goals upon evaluation in Section 3.3:

- (Encoder-level) Enlarging forgetting on  $D_{\text{unlearn}}$ : recall that in Equation (2) the forgetting score FS is measured by the difference between feature similarity on  $D_{\text{unlearn}}$  before/after unlearning with pre-trained model  $g$  and unlearned model  $\hat{g}$ . As the first term is fixed (as  $g$  is given) during unlearning, increasing FS is equal to minimizing the second positive alignment term. For this purpose, we explicitly perform such minimization in our objective function and call it *positive alignment calibration*.
- (Downstream-level) **UA** **TA** < **RA**: enlarging FS alone may also hurt the overall downstream performance on the unlearned model  $\hat{g}$ . To obtain reasonable UA and TA, we find it beneficial to maintain the term for negative pairs in contrastive learning, such that for  $D_{\text{unlearn}}$ , we minimize:

$$L_{\text{unlearn}} = \underbrace{\mathbb{E}_{(x,y) \sim \rho_u^+} s(g(x); g(y))}_{\text{positive alignment calibration}} + \underbrace{\mathbb{E}_x \log \mathbb{E}_y \exp(s(g(x); g(y)))}_{\text{performance preserving}}; \quad (4)$$

where  $\rho_u$  is the density of  $D_{\text{unlearn}}$ . Wang & Isola (2020) states that alignment and uniformity are crucial properties of good representations. While we calibrate alignment with the first term, our performance preserving term implicitly maintains uniformity, which we will demonstrate in Section 5.5.

### 4.2 CALIBRATION UNDER UNLEARNING AUDITING

**Auditing beyond FS:** Recall that in Section 3.3, we show that the forgetting score FS is not a sufficient nor reliable evaluation for unlearning success. Here we introduce an additional auditing tool: given  $D_{\text{unlearn}}$  and the models before unlearning  $g$ , data owners can easily obtain the feature vectors with two different data augmentations:  $g(\mathbf{x}) = fg(x_i)g_{i=1}^{D_{\text{unlearn}}}$  and  $g(\mathbf{y}) = fg(y_j)g_{j=1}^{D_{\text{unlearn}}}$ . Then an Alignment Matrix:  $\text{AM}(g(\mathbf{x}); g(\mathbf{y}))$  can be easily acquired by calculating the pairwise similarity between the two vectors. See Figure 3(a) for some visualizations of AM in the format of heatmaps. Similarly, can obtain  $\text{AM}(\hat{g}(\mathbf{x}); \hat{g}(\mathbf{y}))$  after unlearning and an additional Alignment Gap Matrix:  $\text{AGM} = \text{AM}(g(\mathbf{x}); g(\mathbf{y})) - \text{AM}(\hat{g}(\mathbf{x}); \hat{g}(\mathbf{y}))$ . The heatmaps of AM and AGM provide auditing tools beyond FS and allow to visualize the model change through unlearning by looking at the temperature of the graphs. Notably, the elements on the diagonal of AGM also visualize sample-wise forgetting scores. We direct readers to visualizations of such graphs in Figure 2 and Figure 3 in Section 5.

**Taking auditing into account for unlearning:** The additional auditing tools enable the model owners to design an algorithm that allows data owners to clearly visualize the effect caused by unlearning (*i.e.*, through AM or AGM) without sacrificing the goal of unlearning.

We provide a simple solution to improve existing unlearning methods. As we have explicitly calibrated the alignment of positive pairs of  $L_{\text{unlearn}}$  in Equation (4), it suffices to adjust that of negative pairs (within  $D_{\text{unlearn}}$ ) to a larger value to enlarge the model differences in AM. Specifically, we update the unlearn loss in Equation (4) with *negative alignment calibration*:

$$\underbrace{\mathbb{E}_{(x,y) \sim \rho_u^-} s(g(x); g(y))}_{\text{negative alignment calibration}} + \underbrace{\mathbb{E}_{(x,y) \sim \rho_u^+} s(g(x); g(y))}_{\text{positive alignment calibration}} + \underbrace{\mathbb{E}_x \log \mathbb{E}_y \exp(s(g(x); g(y)))}_{\text{performance preserving}};$$

where  $\alpha, \beta$  are tunable parameters to adjust the strength of each component,  $p_U$  represents negative pairs within the negative set. We write the complete objective of *Alignment Calibration (AC)*:

$$L_{\text{retain}} + \alpha L_{\text{unlearn}} \quad (5)$$

where  $\alpha = |D_{\text{unlearn}}|/|D_{\text{retain}}|$  varies by the size of the unlearn set. In the next section, we will show *AC* not only achieves state-of-the-art performance upon model owners’ evaluations but can also easily pass data owners’ visual auditing on unlearning.

## 5 EXPERIMENT

Recall that we made several claims in Section 3 and Section 4: ¶ Existing methods are suboptimal unlearners under *white-box evaluations* and our *AC* algorithm approaches exact unlearning in this regard; · Under MUC, *AC* introduces alignment matrices *AM* for visual auditing and exhibits clear evidence for unlearning. In this section, we evaluate the baseline methods and *AC* following the above steps and present *white-box evaluation* by model owners and *black-box auditing* by data owners.

### 5.1 EXPERIMENTAL SETUP

**Data and models.** For unimodal contrastive unlearning, we perform experiments on CIFAR-10/CIFAR-100 and SimCLR/MoCo algorithms with the ResNet-18 backbone (we provide additional results on ResNet-50 in Table 9 in Appendix B). We randomly forget 10/50% training data from a pre-trained encoder. For multimodal contrastive unlearning, we evaluate CLIP (Radford et al., 2021) on an Image-Text paired dataset called MS-COCO (Lin et al., 2014), which contains 120K images and 600K captions. We perform unlearning on 10% randomly selected image-text pairs.

**White-box Evaluation:** Following Section 3.3, we use FS and EMIA for encoder-level evaluation, and use CMIA, RA, TA, and UA for downstream-level evaluation after performing linear probing for SimCLR/MoCo experiments. For the evaluation of CLIP, we measure the image-text cosine similarity of the retain dataset and unlearn dataset due to the lack of suitable downstream tasks. Across all experiments, we compare each unlearning method with the exact unlearning (retraining) baseline and report the differences across all metrics. We also report the running time efficiency (RTE) of unlearning methods to evaluate efficiency.

**Black-box Auditing:** Recall that due to the limited access of data owners, the above white-box evaluation can not be directly applied. Instead, we use the *Alignment Matrix (AM)* and *Alignment Gap Matrix (AGM)* introduced in Section 4 for visual auditing on MoCo and CLIP.

**Unlearning Algorithms:** We evaluate Retrain, Fine-Tune, Gradient Ascent, NegGrad, and  $\ell_1$ -Sparsity as baselines for MUC. Our *Alignment Calibration* method updates the pre-trained encoder for the same number of epochs as FineTune, NegGrad, and  $\ell_1$ -Sparsity. For simplicity, we set  $\alpha = \beta = 1$  if not otherwise stated and we tune  $\alpha, \beta$  for the best performance. Implementation details of the above methods are described in Appendix A.2.

### 5.2 UNLEARNING PERFORMANCE UNDER WHITE-BOX EVALUATION

We first provide empirical evidence for model owners to choose a suitable unlearning method with superb efficiency and effectiveness. ¶ Unimodal contrastive learning: We present our evaluation under EMIA, RA, TA, UA and CMIA in Table 1 and Table 2 for unlearning 10/50% of CIFAR-10 training set and FS (CIFAR-10, MoCo) for 10/50% separately in Table 5 due to different scales. We also report the average gap percentage in Appendix B.3. For both SimCLR and MoCo, our proposed *Alignment Calibration (AC)* method achieves the lowest average performance gap over EMIA, RA, TA, UA, and CMIA. In terms of unlearning efficiency, our method only introduces a slight overhead. Additionally, our method achieves the lowest FS gap compared to retraining. In Table 3 and Table 7 in Appendix B, we also report the results on CIFAR-100, where our methods consistently achieve the best performance. · Multi-modal contrastive learning: in Table 4, we again observe that our method is the best approximator of exact unlearning when evaluating the image-text cosine similarity.

Table 1: Unlearning performance of different methods on randomly forgetting 10% of CIFAR-10 training data under various metrics. The performance gaps between retraining and other methods are shown in the parenthesis. We report the average gap (Avg. Gap) over these 5 metrics. The results are obtained by averaging over 5 random trials.

Methods	EMIA	RA	TA	UA	CMIA	Avg. Gap (%) #	RTE (mins) #
MoCo							
Retrain	49.72	89.54	87.76	88.42	34.38	-	109.47
Fine-Tune	50.15 (0.43)	88.34 (1.20)	86.46 (1.30)	87.59 (0.83)	29.42 (4.96)	1.74	1.42
Grad. Ascent	44.95 (4.77)	89.92 (0.38)	88.28 (0.52)	89.76 (1.34)	28.53 (5.85)	2.57	0.17
NegGrad	48.43 (1.29)	89.25 (0.29)	87.35 (0.40)	88.58 (0.16)	28.89 (5.49)	1.53	1.70
$\gamma$ -Sparsity	49.38 (0.34)	88.56 (0.98)	86.91 (0.84)	88.12 (0.30)	29.91 (4.47)	1.39	1.43
Ours	50.28 (0.56)	89.14 (0.40)	87.24 (0.52)	88.20 (0.22)	31.50 (2.88)	<b>0.92</b>	1.87
SIMCLR							
Retrain	48.11	90.87	88.94	89.68	38.87	-	151.77
Fine-Tune	47.72 (0.39)	89.38 (1.49)	87.26 (1.68)	88.93 (0.75)	30.71 (8.16)	2.49	1.93
Grad. Ascent	41.48 (6.63)	91.26 (0.40)	89.55 (0.61)	91.11 (1.43)	29.36 (9.50)	3.71	0.19
NegGrad	49.56 (1.46)	89.10 (1.77)	87.23 (1.71)	89.07 (0.61)	29.97 (8.89)	2.89	2.34
$\gamma$ -Sparsity	48.44 (0.33)	90.59 (0.28)	88.56 (0.38)	90.44 (0.75)	30.61 (8.26)	2.00	1.96
Ours	48.64 (0.53)	90.24 (0.63)	88.06 (0.88)	89.24 (0.44)	33.12 (5.75)	<b>1.65</b>	3.00

Table 2: Unlearning performance of various methods on randomly forgetting 50% of CIFAR-10 training data. The results are averaged over 5 random trials.

Methods	EMIA	RA	TA	UA	CMIA	Avg. Gap (%) #	RTE (mins) #
MoCo							
Retrain	55.95	85.98	83.55	83.98	46.66	-	66.71
Fine-Tune	49.98 (5.97)	87.89 (1.90)	85.66 (2.12)	86.65 (2.67)	32.35 (14.31)	5.39	0.86
Grad. Ascent	42.90 (13.06)	89.51 (3.53)	87.79 (4.25)	88.99 (5.01)	31.85 (14.82)	8.13	0.45
NegGrad	57.40 (1.45)	83.04 (2.94)	80.15 (3.40)	80.59 (3.39)	40.65 (6.02)	3.44	1.66
$\gamma$ -Sparsity	52.19 (3.76)	81.60 (4.38)	80.19 (3.36)	80.77 (3.20)	38.43 (8.24)	4.59	0.87
Ours	55.02 (0.93)	86.28 (0.30)	83.28 (0.26)	83.72 (0.26)	38.39 (8.27)	<b>2.00</b>	1.84
SIMCLR							
Retrain	53.37	87.23	85.16	85.69	49.30	-	89.74
Fine-Tune	45.90 (7.47)	87.88 (0.65)	85.50 (0.34)	87.23 (1.54)	35.44 (13.85)	4.77	1.17
Grad. Ascent	42.23 (11.13)	90.52 (3.28)	88.61 (3.45)	90.45 (4.77)	33.28 (16.02)	7.73	0.59
NegGrad	55.70 (2.33)	83.98 (3.25)	82.15 (3.01)	83.80 (1.89)	33.67 (15.62)	5.22	2.32
$\gamma$ -Sparsity	45.61 (6.86)	89.84 (2.60)	87.75 (2.59)	89.48 (3.80)	35.38 (13.91)	5.95	1.19
Ours	47.12 (6.25)	86.11 (1.13)	83.92 (1.24)	85.24 (0.45)	37.57 (11.72)	<b>4.16</b>	3.07

### 5.3 BLACK-BOX AUDITING

Motivated by the insufficiency of auditing with the FS score, we propose to apply the Alignment Matrix (AM) and Alignment Gap Matrix (AGM) in Section 4. AM and AGM naturally introduce additional quantification of negative alignment. In Figure 2, we report the negative alignment value (mean and standard deviation of pairwise similarity on negative samples in AGM) of 4500 unlearn samples and observe that our method AC exhibits a more significant unlearning effect

Table 3: Unlearning performance of various methods on randomly forgetting 10% of CIFAR-100 training data. The results are averaged over 5 random trials.

Methods	EMIA	RA	TA	UA	CMIA	Avg. Gap (%) #	RTE (mins) #
MoCo							
Retrain	56.24	62.23	58.60	58.43	59.53	-	109.47
Fine-Tune	46.05 (10.19)	63.49 (1.27)	58.88 (0.29)	59.80 (1.37)	48.81 (10.72)	4.77	1.42
Grad. Ascent	44.01 (12.23)	62.56 (0.33)	59.00 (0.41)	60.65 (2.22)	53.28 (6.25)	3.96	0.17
NegGrad	53.58 (2.66)	63.70 (1.47)	58.78 (0.19)	58.85 (0.42)	48.68 (10.84)	3.12	1.70
$\gamma$ -Sparsity	45.68 (10.56)	60.89 (1.34)	57.40 (1.20)	58.66 (0.23)	52.48 (7.04)	4.07	1.43
Ours	50.17 (6.07)	63.20 (0.97)	58.56 (0.04)	58.44 (0.00)	54.15 (5.38)	<b>2.49</b>	1.87
SIMCLR							
Retrain	51.20	57.76	56.25	55.86	65.60	-	151.77
Fine-Tune	40.85 (10.35)	57.29 (0.48)	54.96 (1.29)	55.85 (0.00)	60.61 (4.99)	3.42	1.93
Grad. Ascent	34.00 (17.21)	62.12 (4.36)	59.58 (3.32)	61.08 (5.23)	54.21 (11.39)	8.30	0.19
NegGrad	46.39 (4.81)	56.52 (1.24)	54.30 (1.95)	55.00 (0.86)	60.04 (5.56)	2.89	2.34
$\gamma$ -Sparsity	40.55 (10.66)	57.85 (0.09)	55.76 (0.49)	56.68 (0.83)	58.46 (7.15)	3.84	1.96
Ours	46.72 (4.48)	57.11 (0.65)	54.70 (1.55)	55.23 (0.63)	59.78 (5.83)	<b>2.63</b>	3.00



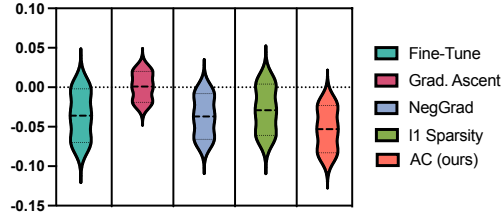
Table 4: Performance of methods on randomly forgetting 10% of MS-COCO data from a pre-trained CLIP. We report the image-text cosine similarity of the retain dataset and unlearn dataset respectively, as well as the average absolute gap from Retrain. The results are averaged over 3 random trials.

Dataset	Pre-train	Retrain	Fine-Tune	Grad. Ascent	NegGrad	$\ell_1$ -Sparsity	Ours
Retrain	62.09	62.47 (0)	58.67 (3.80)	61.96 (0.51)	58.57 (3.90)	57.70 (4.76)	60.75 (1.72)
Unlearn	62.08	49.84 (0)	54.75 (4.91)	62.03 (12.19)	49.19 (0.65)	53.54 (3.70)	51.23 (1.39)
Avg. Gap (%) #	-	0	4.35	6.35	2.28	4.23	<b>1.56</b>

Table 5: Forgetting score (FS) of methods for CIFAR-10 and MoCo. FS gaps are computed between Retrain and other methods.

Methods	10%		50%	
	FS	Gap #	FS	Gap #
Retrain	0.0266	-	0.0604	-
Fine-Tune	0.0393	0.0127	0.0423	0.0180
Grad.Ascent	0.0005	0.0262	0.0007	0.0596
NegGrad	0.0205	0.0061	0.1002	0.0398
$\ell_1$ -Sparsity	0.0216	0.0050	0.0408	0.0195
Ours	0.0259	<b>0.0007</b>	0.0672	<b>0.0068</b>

Figure 2: Negative alignment of 4500 unlearn samples (10%) and MoCo and CIFAR-10. The error bar is the standard deviation.



under such auditing. For individual data owners  $i$ , the size of their subset  $|D_{\text{unlearn}}^i|$  may be small. Therefore, we provide additional qualitative results for visual auditing: we randomly select 8 samples from  $D_{\text{unlearn}}$  to simulate the budget of  $i$ . We construct AM (before/after unlearning with AC) and AGM for this small set and plot their heatmaps in Figure 3 and observe the apparent effect of unlearning. We provide additional results for other methods and CLIP unlearning in Figure 6 and Figure 7 in Appendix B.2, where AC consistently exhibits the best performance under visual auditing.

#### 5.4 ABLATION STUDY

**Influence of negative alignment calibration:** In Equation (5), the coefficient  $\alpha$  controls the intensity of maximizing the negative alignment on unlearn data. To explore the effect of negative alignment calibration in the unlearning task, we fix  $\beta$  and adjust  $\alpha$  while keeping  $\gamma = 1$  for simplicity. Figure 4 (orange bars) reports the ratio between the forgetting score FS of Retrain and AC. When  $\alpha$  increases, the ratio decreases, indicating that the resulting model forgets more information about the unlearn data. A ratio of 1 denotes that the FS of AC equals that of Retrain. Furthermore, we consider a more extreme case of  $\alpha = 0$ , representing no negative calibration. In Table 6, without negative calibration, the average gap over metrics is larger than that of the standard AC by 0.33/2.12% (comparing rows “w/o+w/” with “w/+w/”) for 10/50% forgetting tasks, suggesting this additional term not only benefits the data owner for unlearn auditing but also improves the unlearn performance.

**Influence of positive alignment calibration.** In Equation (5), the coefficient  $\beta$  controls the intensity of minimizing the positive alignment on the unlearn data. In Figure 4 (blue columns), we fix  $\alpha = 1$  and vary  $\beta$  from 0 to 16. The forgetting score ratio decreases with increasing  $\beta$  and

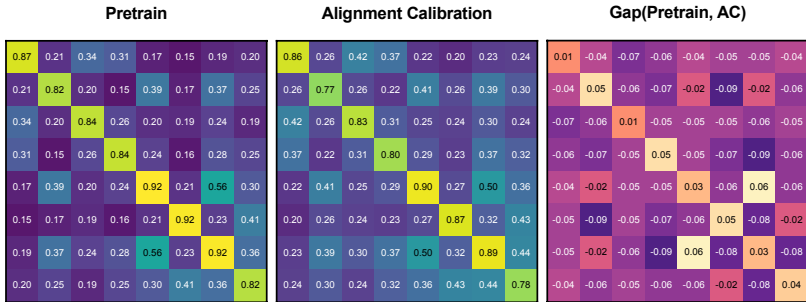


Figure 3: Alignment Matrices and Alignment Gap Matrix on 8 random images in unlearn dataset of CIFAR-10 (MoCo). The task is forgetting 10% of training data.

486  
487  
488  
489  
490  
491  
492  
493  
494  
495  
496  
497  
498  
499  
500  
501  
502  
503  
504  
505  
506  
507  
508  
509  
510  
511  
512  
513  
514  
515  
516  
517  
518  
519  
520  
521  
522  
523  
524  
525  
526  
527  
528  
529  
530  
531  
532  
533  
534  
535  
536  
537  
538  
539

Table 6: Ablation study on positive and negative calibration in Equation (5) regarding the average gap over metrics on CIFAR-10 and MoCo with forgetting ratio 10/50%. “w/” denote with and “w/o” denotes without. For example, “w/o + w/” means AC without negative calibration but with positive calibration.

Objectives	Forgetting 10%	50%
w/ + w/	0.92	2.00
w/o + w/	1.25	4.12
w/ + w/o	1.95	3.75
w/o + w/o	2.70	6.45

approximately reaches 1.0 in the range of [12,16]. In Table 6, the positive alignment calibration term enhances the unlearning performance from 1.95/3.75% to 0.92/2% (comparing columns “w/+w/o” with “w/+w/”) for the 10/50% forgetting tasks regarding the average gap.

## 5.5 PRESERVING UNIFORMITY

Finally, we validate the function of the performance preserving term in our loss function, which forces extracted features to spread uniformly on the hyper-sphere. Following the implementation from Wang & Isola (2020), we visualize the uniformity of features on CIFAR-10 before and after applying our AC unlearning algorithm. Specifically, we train a ResNet-18 encoder mapping images to 2D space using SimCLR and plot the distribution of angles  $\theta = \arctan2(x, y)$  for each point  $(x, y) \in S^1$  in Figure 5. We observe that this term implicitly maintains the uniformity of the representation on both the test dataset and the unlearn dataset.

Before AC                      = 0                      = 2                      = 5                      = 10

(a) Test dataset

(b) Unlearn dataset

Figure 5: Angle distributions on test dataset and unlearn dataset before and after AC unlearning with different  $\alpha$  values related to positive alignment calibration intensity. Here, the negative alignment calibration and performance-preserving term intensities are kept at their default values  $\beta = \gamma = 1$ . Note that when  $\alpha = 0$ , only negative alignment calibration and performance-preserving terms take effect in our AC method. Each chart’s x-axis represents “Angles” and the y-axis represents “Counts”.

## 6 CONCLUSION

In this paper, we study the problem of machine unlearning for contrastive learning pre-training (MUC). We establish the foundations on this line of study by adapting existing unlearning methods and setting up baseline evaluation metrics, including white-box evaluation for model owners to choose an optimal unlearning strategy, and black-box auditing for data owners to examine the effect of unlearning. After identifying the suboptimality of existing unlearning methods and the insufficiency of current auditing tools, we further propose our novel method called Alignment Calibration. Our approach introduces a novel unlearning objective function to strategically optimize toward the unlearning goal and enable straightforward visual auditing. Empirically, our method achieves state-of-the-art performance on unlearning tasks for both unimodal and multimodal contrastive learning. Our paper initializes the study of machine unlearning in self-supervised learning but only considers contrastive learning. We plan to extend our exploration of unlearning towards other SSL methods in the future.

## REFERENCES

- 540  
541  
542 Josh Achiam, Steven Adler, Sandhini Agarwal, Lama Ahmad, Ilge Akkaya, Florencia Leoni Aleman,  
543 Diogo Almeida, Janko Altschmidt, Sam Altman, Shyamal Anadkat, et al. Gpt-4 technical report.  
544 arXiv preprint arXiv:2303.08774, 2023.
- 545 Lucas Bourtole, Varun Chandrasekaran, Christopher A Choquette-Choo, Hengrui Jia, Adelin Travers,  
546 Baiwu Zhang, David Lie, and Nicolas Papernot. Machine unlearning. 2021 IEEE Symposium  
547 on Security and Privacy (SP), pp. 141–159. IEEE, 2021. URL [https://ieeexplore.ieee.  
548 org/iel7/9519381/9519382/09519428.pdf](https://ieeexplore.ieee.org/iel7/9519381/9519382/09519428.pdf)
- 549 Yinzhi Cao and Junfeng Yang. Towards making systems forget with machine unlearning. In  
550 IEEE symposium on security and privacy, pp. 463–480. IEEE, 2015.
- 551 Mathilde Caron, Hugo Touvron, Ishan Misra, Hervé Jegou, Julien Mairal, Piotr Bojanowski, and  
552 Armand Joulin. Emerging properties in self-supervised vision transformers. Proceedings of the  
553 IEEE/CVF international conference on computer vision, pp. 9650–9660, 2021.
- 554 Min Chen, Weizhuo Gao, Gaoyang Liu, Kai Peng, and Chen Wang. Boundary unlearning:  
555 Rapid forgetting of deep networks via shifting the decision boundary. Proceedings of  
556 the IEEE/CVF Conference on Computer Vision and Pattern Recognition, pp. 7766–7775,  
557 2023. URL [http://openaccess.thecvf.com/content/CVPR2023/papers/  
558 Chen\\_Boundary\\_Unlearning\\_Rapid\\_Forgetting\\_of\\_Deep\\_Networks\\_via\\_  
559 Shifting\\_the\\_CVPR\\_2023\\_paper.pdf](http://openaccess.thecvf.com/content/CVPR2023/papers/Chen_Boundary_Unlearning_Rapid_Forgetting_of_Deep_Networks_via_Shifting_the_CVPR_2023_paper.pdf)
- 560 Ting Chen, Simon Kornblith, Mohammad Norouzi, and Geoffrey Hinton. A simple framework for  
561 contrastive learning of visual representations. ICLR, 2020. URL [http://proceedings.  
562 mlr.press/v119/chen20j.html](http://proceedings.mlr.press/v119/chen20j.html)
- 563 Xinlei Chen and Kaiming He. Exploring simple siamese representation learning. Proceedings of  
564 the IEEE/CVF Conference on Computer Vision and Pattern Recognition, pp. 15750–15758, 2021.
- 565 Xinlei Chen, Saining Xie, and Kaiming He. An empirical study of training self-supervised vision  
566 transformers. In Proceedings of the IEEE/CVF International Conference on Computer Vision,  
567 pp. 9640–9649, 2021.
- 568 Ronen Eldan and Mark Russinovich. Who's harry potter? approximate unlearning in dnn.  
569 preprint arXiv:2310.02238, 2023. URL <https://arxiv.org/abs/2310.02238>
- 570 Chongyu Fan, Jiancheng Liu, Yihua Zhang, Eric Wong, Dennis Wei, and Sijia Liu. Salun: Em-  
571 powering machine unlearning via gradient-based weight saliency in both image classification and  
572 generation. In The Twelfth International Conference on Learning Representations, 2024. URL  
573 <https://openreview.net/forum?id=gn0mlhQGNM>
- 574 Rohit Gandikota, Joanna Materzynska, Jaden Fiotto-Kaufman, and David Bau. Erasing concepts  
575 from diffusion models. arXiv preprint arXiv:2303.07345, 2023.
- 576 Antonio Ginart, Melody Guan, Gregory Valiant, and James Y Zou. Making ai forget you: Data  
577 deletion in machine learning. Advances in neural information processing systems, 2019.
- 578 Aditya Golatkar, Alessandro Achille, and Stefano Soatto. Eternal sunshine of the spotless net:  
579 Selective forgetting in deep networks. Proceedings of the IEEE/CVF Conference on Computer  
580 Vision and Pattern Recognition, pp. 9304–9312, 2020. URL [https://openaccess.thecvf.  
581 com/content\\_CVPR\\_2020/papers/Golatkar\\_Eternal\\_Sunshine\\_of\\_the\\_  
582 Spotless\\_Net\\_Selective\\_Forgetting\\_in\\_Deep\\_CVPR\\_2020\\_paper.pdf](https://openaccess.thecvf.com/content_CVPR_2020/papers/Golatkar_Eternal_Sunshine_of_the_Spotless_Net_Selective_Forgetting_in_Deep_CVPR_2020_paper.pdf)
- 583 Jean-Bastien Grill, Florian Strub, Florent Altch, Corentin Tallec, Pierre Richemond, Elena  
584 Buchatskaya, Carl Doersch, Bernardo Avila Pires, Zhaohan Guo, Mohammad Gheshlaghi Azar,  
585 et al. Bootstrap your own latent—a new approach to self-supervised learning. Advances in Neural  
586 Information Processing Systems, pp. 21271–21284, 2020.
- 587 Chuan Guo, Tom Goldstein, Awni Hannun, and Laurens Van Der Maaten. Certified data removal  
588 from machine learning models. arXiv preprint arXiv:1911.03030, 2019.

- 594 Kaiming He, Haoqi Fan, Yuxin Wu, Saining Xie, and Ross Girshick. Momentum contrast for  
595 unsupervised visual representation learning. *CVPR*, 2020.
- 596 Kaiming He, Xinlei Chen, Saining Xie, Yanghao Li, Piotr Dollár, and Ross Girshick. Masked  
597 autoencoders are scalable vision learners. *Proceedings of the IEEE/CVF conference on computer  
598 vision and pattern recognition*, pp. 16000–16009, 2022.
- 600 Alvin Heng and Harold Soh. Selective amnesia: A continual learning approach to forgetting in deep  
601 generative models, 2023.
- 602 Xinshuo Hu, Dongfang Li, Baotian Hu, Zihao Zheng, Zhenyu Liu, and Min Zhang. Separate the  
603 wheat from the chaff: Model de cency unlearning via parameter-ef cient module operation. In  
604 *Proceedings of the AAAI Conference on Arti cial Intelligence*, pp. 18252–18260, 2024. URL  
605 <https://arxiv.org/abs/2308.08090>
- 606 Zachary Izzo, Mary Anne Smart, Kamalika Chaudhuri, and James Zou. Approximate data deletion  
607 from machine learning models. *International Conference on Arti cial Intelligence and Statis-  
608 tics*, pp. 2008–2016. PMLR, 2021. URL [https://proceedings.mlr.press/v130/  
609 izzo21a/izzo21a.pdf](https://proceedings.mlr.press/v130/izzo21a/izzo21a.pdf)
- 611 Joel Jang, Dongkeun Yoon, Sohee Yang, Sungmin Cha, Moontae Lee, Lajanugen Logeswaran, and  
612 Minjoon Seo. Knowledge unlearning for mitigating privacy risks in language models. *arXiv  
613 preprint arXiv:2210.01504*, 2022. URL <https://arxiv.org/abs/2210.01504>
- 614 Jinghan Jia, Jiancheng Liu, Parikshit Ram, Yuguang Yao, Gaowen Liu, Yang Liu, Pranay Sharma,  
615 and Sijia Liu. Model sparsity can simplify machine unlearning. *Thirty-seventh Conference on  
616 Neural Information Processing Systems*, 2023. URL [https://openreview.net/forum?  
617 id=0jZH883i34](https://openreview.net/forum?id=0jZH883i34)
- 618 Jinghan Jia, Yihua Zhang, Yimeng Zhang, Jiancheng Liu, Bharat Runwal, James Diffenderfer,  
619 Bhavya Kaikhura, and Sijia Liu. Soul: Unlocking the power of second-order optimization for llm  
620 unlearning. *arXiv preprint arXiv:2404.18239*, 2024.
- 622 Nupur Kumari, Bingliang Zhang, Sheng-Yu Wang, Eli Shechtman, Richard Zhang, and Jun-Yan Zhu.  
623 Ablating concepts in text-to-image diffusion models, 2023.
- 624 Meghdad Kurmanji, Peter Trianta Ilou, Jamie Hayes, and Eleni Trianta Ilou. Towards unbounded  
625 machine unlearning. In *Thirty-seventh Conference on Neural Information Processing Systems  
626 2023*. URL <https://openreview.net/forum?id=OveBaTtUAT>
- 628 Tsung-Yi Lin, Michael Maire, Serge Belongie, James Hays, Pietro Perona, Deva Ramanan, Piotr  
629 Dollár, and C Lawrence Zitnick. Microsoft coco: Common objects in context. *Computer Vision–  
630 ECCV 2014: 13th European Conference, Zurich, Switzerland, September 6-12, 2014, Proceedings,  
631 Part V 13* pp. 740–755. Springer, 2014. URL <https://cocodataset.org/>
- 632 Hongbin Liu, Jinyuan Jia, Wenjie Qu, and Neil Zhenqiang Gong. Encodermi: Membership inference  
633 against pre-trained encoders in contrastive learning. *Proceedings of the 2021 ACM SIGSAC  
634 Conference on Computer and Communications Security*, pp. 2081–2095, 2021. URL [https:  
635 //dl.acm.org/doi/pdf/10.1145/3460120.3484749](https://dl.acm.org/doi/pdf/10.1145/3460120.3484749)
- 636 Sijia Liu, Yuanshun Yao, Jinghan Jia, Stephen Casper, Nathalie Baracaldo, Peter Hase, Xiaojun Xu,  
637 Yuguang Yao, Hang Li, Kush R Varshney, et al. Rethinking machine unlearning for large language  
638 models. *arXiv preprint arXiv:2402.08787*, 2024.
- 640 Yiwei Lu, Guojun Zhang, Sun Sun, Hongyu Guo, and Yaoliang Yu. Mucicl: Understanding and  
641 generalizing infonce-based contrastive learning transactions on Machine Learning Research  
642 2023.
- 643 Pratyush Maini, Zhili Feng, Avi Schwarzschild, Zachary C Lipton, and J Zico Kolter. Tofu: A task of  
644 cititious unlearning for llms. *arXiv preprint arXiv:2401.06121*, 2024.
- 646 Eric Mitchell, Charles Lin, Antoine Bosselut, Chelsea Finn, and Christopher D Manning. Fast  
647 model editing at scale. *International Conference on Learning Representations*, 2022a. URL  
<https://openreview.net/forum?id=0DcZxeWfOPT>

- 648 Eric Mitchell, Charles Lin, Antoine Bosselut, Christopher D Manning, and Chelsea Finn. Memory-  
649 based model editing at scale. *International Conference on Machine Learning*, pp. 15817–15831.  
650 PMLR, 2022b. URL <https://arxiv.org/abs/2206.06520>
- 651 Seth Neel, Aaron Roth, and Saeed Shari -Malvajerdi. Descent-to-delete: Gradient-based methods  
652 for machine unlearning. *Algorithmic Learning Theory*, pp. 931–962. PMLR, 2021.
- 653 Alec Radford, Jong Wook Kim, Chris Hallacy, Aditya Ramesh, Gabriel Goh, Sandhini Agarwal,  
654 Girish Sastry, Amanda Askell, Pamela Mishkin, Jack Clark, et al. Learning transferable visual  
655 models from natural language supervision. *International conference on machine learning*, pp.  
656 8748–8763. PMLR, 2021.
- 657 Robin Rombach, Andreas Blattmann, Dominik Lorenz, Patrick Esser, and Björn Ommer. High-  
658 resolution image synthesis with latent diffusion models. *Proceedings of the IEEE/CVF confer-  
659 ence on computer vision and pattern recognition*, pp. 10684–10695, 2022.
- 660 Nikunj Saunshi, Orestis Plevrakis, Sanjeev Arora, Mikhail Khodak, and Hrishikesh Khandeparkar.  
661 A theoretical analysis of contrastive unsupervised representation learning. *ICML*, 2019. URL  
662 <http://proceedings.mlr.press/v97/saunshi19a.html>
- 663 Christoph Schuhmann, Romain Beaumont, Richard Vencu, Cade Gordon, Ross Wightman, Mehdi  
664 Cherti, Theo Coombes, Aarush Katta, Clayton Mullis, Mitchell Wortsman, et al. Laion-5b: An  
665 open large-scale dataset for training next generation image-text models. *Advances in Neural  
666 Information Processing Systems*, 35:25278–25294, 2022. URL [https://arxiv.org/abs/  
667 2210.08402](https://arxiv.org/abs/2210.08402)
- 668 Ayush Sekhari, Jayadev Acharya, Gautam Kamath, and Ananda Theertha Suresh. Remember  
669 what you want to forget: Algorithms for machine unlearning. *Advances in Neural Information  
670 Processing Systems*, 34:18075–18086, 2021.
- 671 Shaofei Shen, Chenhao Zhang, Yawen Zhao, Alina Bialkowski, Weitong Tony Chen, and Miao  
672 Xu. Label-agnostic forgetting: A supervision-free unlearning in deep models. *The Twelfth  
673 International Conference on Learning Representations*, 2024. URL [https://openreview.  
674 net/forum?id=SIZWiya7FE](https://openreview.net/forum?id=SIZWiya7FE)
- 675 Liwei Song and Prateek Mittal. Systematic evaluation of privacy risks of machine learning models.  
676 In *30th USENIX Security Symposium (USENIX Security 21)*, pp. 2615–2632, 2021. URL [https:  
677 //www.usenix.org/system/files/sec21fall-song.pdf](https://www.usenix.org/system/files/sec21fall-song.pdf)
- 678 Anvith Thudi, Hengrui Jia, Iliia Shumailov, and Nicolas Papernot. On the necessity of auditable  
679 algorithmic definitions for machine unlearning. *31st USENIX Security Symposium (USENIX  
680 Security 22)*, pp. 4007–4022, 2022. URL [https://www.usenix.org/system/files/  
681 sec22-thudi.pdf](https://www.usenix.org/system/files/sec22-thudi.pdf)
- 682 Christopher Tosh, Akshay Krishnamurthy, and Daniel Hsu. Contrastive learning, multi-view redun-  
683 dancy, and linear models. *Algorithmic Learning Theory*, PMLR, 2021.
- 684 Yao-Hung Hubert Tsai, Martin Q Ma, Muqiao Yang, Han Zhao, Louis-Philippe Morency, and Ruslan  
685 Salakhutdinov. Self-supervised representation learning with relative predictive coding. *ICLR*,  
686 2021.
- 687 Enayat Ullah, Tung Mai, Anup Rao, Ryan A Rossi, and Raman Arora. Machine unlearning via  
688 algorithmic stability. In *Conference on Learning Theory*, pp. 4126–4142. PMLR, 2021.
- 689 Aaron van den Oord, Yazhe Li, and Oriol Vinyals. Representation learning with contrastive predictive  
690 coding. *arXiv preprint arXiv:1807.03748*, 2018.
- 691 Tongzhou Wang and Phillip Isola. Understanding contrastive representation learning through align-  
692 ment and uniformity on the hypersphere. *ICML*. PMLR, 2020.
- 693 Wenhao Wang, Muhammad Ahmad Kaleem, Adam Dziedzic, Michael Backes, Nicolas Papernot, and  
694 Franziska Boenisch. Memorization in self-supervised learning improves downstream generalization.  
695 In *The Twelfth International Conference on Learning Representations*, 2024. URL [https:  
696 //openreview.net/forum?id=KSjPaXtxP8](https://openreview.net/forum?id=KSjPaXtxP8)

702 Yunzhi Yao, Peng Wang, Bozhong Tian, Siyuan Cheng, Zhoubo Li, Shumin Deng, Huajun Chen,  
703 and Ningyu Zhang. Editing large language models: Problems, methods, and opportunities.  
704 In The 2023 Conference on Empirical Methods in Natural Language Processing. URL  
705 <https://openreview.net/forum?id=NZZB3UGcd8>.  
706

707 Dawen Zhang, Pamela Finckenberg-Broman, Thong Hoang, Shidong Pan, Zhenchang Xing, Mark  
708 Staples, and Xiwei Xu. Right to be forgotten in the era of large language models: Implications,  
709 challenges, and solutions. arXiv preprint arXiv:2307.03941, 2023a. URL <https://arxiv.org/abs/2307.03941>.  
710

711 Eric Zhang, Kai Wang, Xingqian Xu, Zhangyang Wang, and Humphrey Shi. Forget-me-not: Learning  
712 to forget in text-to-image diffusion models. arXiv preprint arXiv:2303.17591, 2023b.  
713

714 Qiuchen Zhang, Carl Yang, Jian Lou, Li Xiong, et al. Contrastive unlearning: A contrastive approach  
715 to machine unlearning. arXiv preprint arXiv:2401.10458, 2024a. URL <https://arxiv.org/html/2401.10458v1>.  
716

717 Ruiqi Zhang, Licong Lin, Yu Bai, and Song Mei. Negative preference optimization: From catastrophic  
718 collapse to effective unlearning. arXiv preprint arXiv:2404.05868, 2024b.  
719  
720  
721  
722  
723  
724  
725  
726  
727  
728  
729  
730  
731  
732  
733  
734  
735  
736  
737  
738  
739  
740  
741  
742  
743  
744  
745  
746  
747  
748  
749  
750  
751  
752  
753  
754  
755

## A EXPERIMENT DETAILS

### A.1 DATASETS

CIFAR-10/100. Both datasets consist of 50K training images and 10K test images. All the images are 32x32 colored. CIFAR-100 has 100 categories and CIFAR-10 has 10 categories. In unimodal contrastive learning, the augmentations for training encoders include random resizing and cropping, random grayscale, random color jitter, and horizontal flipping. We split the 50K training images into a validation set of 5K images and a training set of 45K images. For example, when the unlearning task is to forget 10% of training data, the unlearned dataset  $D_{\text{unlearn}}$  has 4.5K images and the retained dataset  $D_{\text{retain}}$  has 4.05K images.

MS-COCO. COCO is a large-scale object detection, segmentation, and captioning dataset. Its training set contains 118,287 images and 591,753 captions. Each image has several objects and corresponds to at least 5 captions. Different from unimodal contrastive learning which uses strong augmentations, CLIP employs only resizing, center cropping and horizontal flipping to make images of 224x224 pixels.

### A.2 CONTRASTIVE LEARNING AND UNLEARNING METHODS

MoCo and SimCLR: For the pre-trained (clean) models, we train the encoder for 800 epochs using an SGD optimizer with cosine-scheduled learning rate initialized at 0.06, momentum of 0.9, and weight decay of 0.0005. For unlearning method Retrain applies the same training strategy as pre-training; Fine-tuning and NegGrad updates the pre-trained encoder for 10 epochs with a learning rate searched in [0.003, 0.03]; Gradient Ascent updates the pre-trained encoder using reversed stochastic gradient descent for 5 epochs with a learning rate searched in  $[10^{-4}, 10^{-1}]$ ; Sparsity applies the learning rate as 0.006 and implements regularization with a coefficient searched in  $[10^{-6}, 10^{-3}]$ . For our Alignment Calibration method, we update the pre-trained encoder for 10 epochs and search the learning rate in [0.003, 0.03] and the tunable parameter  $\alpha$  in [0, 20] for different unlearning tasks. If not otherwise stated, we adopt  $\alpha = 1$ . For simplicity, in our reported results on CIFAR-10/100, we use a learning rate of 0.006 for 10% forgetting, and 0.02 for 50% forgetting. The linear probing stage trains a linear classifier head for 100 epochs using an SGD optimizer with a cosine-scheduled learning rate initialized at 1.0, and a momentum of 0.9. The batch size is set as 512 for both encoder and linear head training.

CLIP: For the pre-trained (clean) CLIP, we train the model for 35 epochs on 2 NVIDIA RTX 4090 GPUs using an AdamW optimizer with a warm-up cosine-scheduled learning rate initialized at  $5e-4$  and momentum of 0.9. The total batch size is 256 (128 on each GPU). For unlearning algorithms: Retrain again applies the same training strategy as pre-training; Fine-tuning update the pre-trained model for 8 epochs with a fixed learning rate searched in  $[5e-5, 5e-4]$ ; NegGrad updates the pre-trained model for 8 epochs with a fixed learning rate searched in  $[10^{-6}, 10^{-4}]$ ; Gradient Ascent updates the pre-trained model for 4 epochs with a fixed learning rate searched in  $[5e-6, 5e-3]$ ; Sparsity updates the pre-trained model for 8 epochs with a learning rate of 0.0005 and a regularization coefficient searched in  $[10^{-9}, 10^{-4}]$ . For our Alignment Calibration method, we update the pre-trained model for 8 epochs with a fixed learning rate of 0.0002. We search  $\alpha$  in [0.5, 1] and  $\beta$  in [0, 1].

### A.3 UNLEARNING EVALUATION

CMIA efficacy. Given an unlearned encoder, we execute linear probing on it and denote the whole classifier by  $f$ . Following the implementation of Jia et al. (2023); Fan et al. (2024), we evaluate the attack successful rate (ASR) on the unlearned dataset  $D_{\text{unlearn}}$  of a confidence-based membership inference attack (Song & Mittal, 2021) to The formal definition of CMIA efficacy is given by:

$$\text{CMIA-Efficacy} := \frac{T_{\text{CMIA}}}{|D_{\text{unlearn}}|}; \quad (6)$$

where  $T_{\text{CMIA}}$  is the number of true negatives predicted by the CMIA attack.

EMIA efficacy. We implement the alignment-based EncoderMI-T attack (Liu et al., 2021) in an adapted white-box setting. Given an unlearned encoder with its retain dataset  $D_{retain}$  and test dataset  $D_{test}$ , we denote  $D_{non-member} := D_{test}$  sample a subset  $D_{member}$  of  $D_{retain}$  such that  $|D_{non-member}| = |D_{member}|$ . For each data  $i \in D_{non-member}$  and  $j \in D_{member}$ , we first augment it 10 times and compute features of these 10 views. Then, we compute the cosine similarity between each pair of features, i.e., 45 pairs, and take the average of these similarity values. Now we get a membership feature dataset and a non-membership feature dataset whose data points are just scalar values. The EncoderMI-T attack then searches for an optimal threshold to classify membership features and non-membership features. Similar to MIA efficacy, the formal definition of EMIA efficacy is given by:

$$EMIA\text{-Efficacy} := \frac{TN_{EMIA}}{|D_{unlearn}|}; \tag{7}$$

where  $TN_{EMIA}$  is the number of true negatives predicted by the EncoderMI attack.

## B ADDITIONAL EXPERIMENTS

### B.1 UNLEARNING PERFORMANCE FOR MORE TASKS

We present experiment results on CIFAR-100 in Tables 3 and 7. Across these different tasks, our proposed Alignment Calibration method achieves the lowest average gap compared to the Retrain method.

Table 7: Performance of methods on randomly forgetting 50% of CIFAR-100 training data. EMIA is evaluated on the unlearned encoder, while RA, TA, UA, and MIA are evaluated after linear probing. We report the average gap (Avg. Gap) over these 5 metrics between methods and Retrain. The results are averaged over 5 random trials.

Methods	EMIA	RA	TA	UA	CMIA	Avg. Gap	RTE
MoCo							
Retrain	60.40	57.72	52.58	52.32	67.30	-	66.71
Fine-Tune	53.58 (6.81)	61.9 (4.18)	56.07 (3.48)	56.87 (4.55)	52.27 (15.03)	6.81	10.86
Grad. Ascent	43.76 (16.63)	60.91 (3.19)	56.2 (3.62)	57.48 (5.16)	55.64 (11.66)	8.05	0.45
NegGrad	38.95 (21.44)	60.94 (3.22)	57.01 (4.43)	58.21 (5.89)	57.64 (9.66)	8.93	1.66
$\ell_1$ -Sparsity	49.97 (10.43)	58.89 (1.17)	53.07 (0.49)	53.66 (1.33)	56.27 (11.03)	4.89	0.87
Ours	56.22 (4.18)	59.53 (1.81)	53.37 (0.79)	53.69 (1.37)	52.27 (15.03)	4.63	1.84
SIMCLR							
Retrain	56.00	50.40	48.46	47.68	69.47	-	89.74
Fine-Tune	53.89 (2.12)	52.82 (2.42)	49.87 (1.41)	51.04 (3.36)	60.06 (9.41)	3.74	1.17
Grad. Ascent	40.28 (15.72)	56.32 (5.92)	54.12 (5.66)	55.22 (7.54)	61.43 (8.04)	8.58	0.59
NegGrad	46.83 (9.17)	50.60 (0.20)	48.20 (0.26)	49.29 (1.62)	58.01 (11.47)	4.54	2.32
$\ell_1$ -Sparsity	45.12 (10.89)	52.62 (2.22)	50.09 (1.62)	50.98 (3.30)	65.25 (4.22)	4.45	1.19
Ours	54.98 (1.02)	49.28 (1.12)	46.8 (1.66)	47.00 (0.68)	57.78 (11.69)	3.24	3.07

### B.2 MORE VISUAL AUDITING RESULTS

In Figure 6, we report the AGP of Retrain, Fine-Tune, Gradient Ascent, NegGradSparsity on CIFAR-10, as a complement to Figure 3. For the unlearning task on CLIP, we check our AC and other baseline methods in Figure 7.

### B.3 COMPARISON USING AVERAGE GAP PERCENTAGE STANDARD

In previous experiments, we compare our AC and baseline methods using the average gap across multiple metrics. To comprehensively illustrate the advantage of our method, we introduce a different standard for comparison, average gap percentage (AGP), which averages the percentage of GAP over Retrain across multiple metrics. In Table 8, we perform unlearning tasks of forgetting 10%/50% of CIFAR-10 data from ResNet-18 SimCLR/MoCo encoders and our proposed AC method still outperforms baseline methods concerning the AGP standard.



864  
865  
866  
867  
868  
869  
870  
871  
872

Figure 6: Alignment Gap Matrices of 8 unlearn images for Retrain, Fine-Tune, Gradient Ascent, NegGrad,  $\ell_1$ -Sparsity, and Alignment Calibration. The unlearning task is to forget 10% of CIFAR-10 training data from a MoCo encoder.

876  
877  
878  
879  
880  
881  
882  
883  
884  
885

Figure 7: Alignment Gap Matrices of 6 unlearn image-text pairs for Retrain, Fine-Tune (FT), Gradient Ascent (GA), NegGrad (NG),  $\ell_1$ -Sparsity, and Alignment Calibration (AC). The unlearning task is to forget 10% of MS-COCO training data from a CLIP encoder.

889  
890  
891  
892

Table 8: Comparison in average gap percentage (AGP, %) with other baseline methods. AGP averages the percentages of Gap over Retrain, e.g.,  $\text{MEAN}(\frac{\text{gap}}{\text{retrain}})$ . Table 9: Unlearning performance of randomly forgetting 10% of CIFAR-10 training data from ResNet-50 MoCo encoders. We compare AC with baseline methods in Average Gap (AG, %) and the Average Gap Percentage (AGP, %).

CIFAR-10	10%		50%		EMIA	RA	TA	UA	CMIA	AG	AGP
	MoCo	SimCLR	MoCo	SimCLR							
Retrain					53.56	92.10	90.10	90.98	35.44	-	-
Fine-Tune	3.81	5.23	9.85	9.01	49.85	91.74	89.64	91.04	23.92	4.68	8.07
Grad. Ascent	5.83	8.19	14.05	13.35	39.36	92.36	90.71	92.32	25.37	4.43	11.49
NegGrad	3.91	6.09	5.40	9.10	52.62	91.85	89.78	90.64	24.82	0.07	6.51
$\ell_1$ -Sparsity	3.22	4.70	7.46	10.31	47.61	90.54	88.67	90.19	27.04	3.63	7.79
AC (ours)	2.16	3.61	4.07	7.75	53.48	91.75	89.32	89.82	30.56	1.45	3.29

899  
900  
901  
902  
903  
904  
905  
906  
907

Table 10: Performance of methods on randomly forgetting 10% of SVHN training data from a pre-trained MoCo encoder. The results are averaged over 5 random trials.

Methods	EMIA	RA	TA	UA	CMIA	Avg. Gap	RTE
Retrain	51.24	91.17	92.02	90.59	20.46	-	114.13
Fine-Tune	50.69 (0.54)	90.19 (0.98)	90.63 (1.39)	89.75 (0.84)	17.03 (3.43)	1.44	1.41
Grad. Ascent	46.45 (4.79)	91.23 (0.06)	92.25 (0.22)	90.94 (0.35)	18.44 (2.02)	1.49	0.17
NegGrad	50.99 (0.24)	90.67 (0.50)	91.14 (0.88)	90.08 (0.50)	17.42 (3.03)	1.03	1.74
$\ell_1$ -Sparsity	50.56 (0.67)	89.20 (1.97)	89.72 (2.31)	88.89 (1.70)	20.52 (0.06)	1.34	1.45
Ours	51.50 (0.26)	90.19 (0.98)	90.76 (1.27)	89.23 (1.36)	19.99 (0.46)	0.87	1.98

916  
917

Table 11: Standard deviation for Tables 1 to 3. Appendix B.6 shows the detailed settings for random trials.

	EMIA	RA	TA	UA	CMIA	EMIA	RA	TA	UA	CMIA
	CIFAR-10, 10%, MoCo					CIFAR-10, 50%, MoCo				
Retrain	49.72±5.58	89.54±0.07	87.76±0.25	88.42±0.66	34.38±0.83	55.95±1.58	85.98±0.25	83.55±0.27	83.98±0.21	46.66±0.73
Fine-Tune	50.15±7.99	88.34±0.27	86.46±0.13	87.59±0.18	29.42±1.37	49.98±2.92	87.89±0.55	85.66±0.43	86.65±0.29	32.35±0.90
Grad. Ascent	44.95±6.61	89.92±0.16	88.28±0.23	89.76±0.46	28.53±0.76	42.90±5.46	89.51±0.30	87.79±0.24	88.99±0.17	31.85±0.61
NegGrad	48.43±5.42	89.25±0.24	87.35±0.23	88.58±0.49	28.89±0.86	57.40±3.24	83.04±0.47	80.15±0.71	80.59±0.56	40.65±0.02
1-Sparsity	49.38±7.15	88.56±0.32	86.91±0.40	88.12±0.39	29.91±0.92	52.19±6.71	81.60±0.76	80.19±0.91	80.77±0.81	38.43±6.48
Ours	50.28±5.86	89.14±0.19	87.24±0.25	88.20±0.50	31.50±1.17	55.02±5.14	86.28±0.35	83.28±0.37	83.72±0.26	38.39±1.27
	CIFAR-10, 10%, SimCLR					CIFAR-10, 50%, SimCLR				
Retrain	48.11±3.70	90.87±0.08	88.94±0.16	89.68±0.33	38.87±1.33	53.37±2.21	87.23±0.25	85.16±0.34	85.69±0.17	49.30±0.65
Fine-Tune	47.72±4.38	89.38±0.51	87.26±0.65	88.93±0.56	30.71±1.61	45.90±3.25	87.88±0.34	85.50±0.34	87.23±0.30	35.44±1.50
Grad. Ascent	41.48±1.51	91.26±0.13	89.55±0.37	91.11±0.36	29.36±0.99	42.23±1.50	90.52±0.28	88.61±0.15	90.45±0.16	33.28±2.47
NegGrad	49.56±3.95	89.10±0.32	87.23±0.45	89.07±0.43	29.97±1.13	55.70±3.70	83.98±0.90	82.15±0.68	83.80±0.55	33.67±5.75
1-Sparsity	48.44±6.70	90.59±0.23	88.56±0.30	90.44±0.28	30.61±1.01	46.51±3.85	89.84±0.12	87.75±0.28	89.48±0.22	35.38±1.52
Ours	48.64±4.47	90.24±0.11	88.06±0.23	89.24±0.30	33.12±1.54	47.12±5.84	86.11±0.31	83.92±0.30	85.24±0.60	37.57±1.16
	CIFAR-100, 10%, MoCo					CIFAR-100, 10%, SimCLR				
Retrain	56.24±2.77	62.23±0.27	58.60±0.28	58.43±0.64	59.53±1.57	51.20±2.07	57.76±0.30	56.25±0.31	55.86±0.78	65.60±1.70
Fine-Tune	46.05±4.96	63.49±0.56	58.88±0.44	59.80±0.91	48.81±1.21	40.85±3.81	57.29±0.13	54.96±0.43	55.85±1.04	60.61±3.70
Grad. Ascent	44.01±2.70	62.56±0.11	59.00±0.06	60.65±0.64	53.28±2.12	34.00±3.81	62.12±0.25	59.58±0.22	61.08±0.61	54.21±1.91
NegGrad	53.58±1.82	63.70±0.25	58.78±0.27	58.85±0.53	48.68±2.02	46.39±5.10	56.52±0.52	54.30±0.67	55.00±1.08	60.04±3.13
1-Sparsity	45.68±7.30	60.89±0.41	57.40±0.59	58.66±0.78	52.48±3.21	40.55±3.43	57.85±0.24	55.76±0.34	56.68±0.64	58.46±6.10
Ours	50.17±3.42	63.20±0.37	58.56±0.59	58.44±0.42	54.15±1.66	46.72±5.50	57.11±0.38	54.70±0.36	55.23±0.91	59.78±5.46

## B.4 MODEL ARCHITECTURE

In Table 9, we perform an unlearning task of forgetting 10% of CIFAR-10 data from a ResNet-50 MoCo encoder. Our AC method outperforms baseline methods concerning both average gap and average gap percentage standards.

## B.5 SVHN RESULTS

In Table 10, we report the unlearning results on the SVHN dataset. Our Alignment Calibration method achieves the least average gap to Retraining compared to the other 4 baseline methods while showing comparable efficiency in the unlearning process.

## B.6 RANDOM TRIAL SETTINGS

Recall that our results in Tables 1 to 3 are averaged results over  $v$  random trials for each unlearning setting. Specifically, we use random seeds 0, 1, 2, 3, and 4. Each random seed determines both the selection of unlearning samples and the corresponding pre-trained and retrained encoders. For instance, with a specific random seed, our AC method and other baseline methods start from the same pre-trained encoder to forget the same samples and aim to approximate the same retrained encoder. The metrics are computed in each random trial. We report the standard deviation for Tables 1 to 3 in Table 11.